

Supporting information

Functionalised Electrospun Membranes (TETA-PVC) for the Removal of Lead(II) from Water

Fatima Youness,^a Amani Jaafar,^a Ali Tehrani,^b and Rana A. Bilbeisi^{*a}

Table of Contents	
List of Figures.....	2
List of tables.....	2
1. General	3
1.1. Chemicals and materials.....	3
1.2. Instruments and methods.....	3
2. Metal-organic complex detection using UV-visible spectroscopy	4
2.1. Metal-organic complex detection.....	4
2.2. Binding isotherm of lead(II) ion and TETA	4
3. Synthesis and functionalisation of PVC membrane	5
4. Characterisation of PVC and TETA-PVC membranes	6
4.1. Fourier-transform infrared spectroscopy.....	6
4.2. Scanning Electron Microscopy.....	7
4.3. Energy Dispersive X-ray.....	8
4.4. Pore size, membrane thickness, and water contact angle measurements.....	8
5. Removal efficiency of Pb(II) ions from water	10
6. Adsorption Kinetics	11
7. Adsorption Isotherm models	12
7.1. Langmuir isotherm model.....	12
7.2. Freundlich isotherm model.....	13
8. Ion selectivity test	14
8.1. Tertiary System.....	14
8.2. Mixed Metal Ions System.....	15
9. Regeneration of TETA-PVC membrane	16
List of References.....	17

List of Figures

Figure S1: Absorption spectrum of **Pb(II)** and **TETA** in aqueous solutions:(a), **lead(II)** acetate trihydrate within the UV-visible region (b) triethylenetetramine within the UV-visible region.....4

Figure S2: UV-visible absorption spectra of 1.71×10^{-4} M solution of **Pb(OAC)₂** in H₂O titrated with, increasing concentrations of **TETA**5

Figure S3: FTIR spectra of **PVC, TETA-PVC, and TETA-PVC-Pb** membranes7

Figure S4: SEM images of electrospun **PVC** nanofibers obtained from different **PVC (g): TETA (mL)** ratios (a) unfunctionalised **PVC** membrane; (b) 1:1, (c) 1:2, and (d) 1:3 ratios.7

Figure S5: SEM images of **PVC** nanofibers membrane and **TETA-PVC** nanofibers membrane with different magnifications: unfunctionalised **PVC** (a) 5 μ m, **TETA-PVC** (b) 20 μ m; (c) 10 μ m; (d) 5 μ m. EDX analysis of (e) **PVC** membrane; (f) **TETA-PVC** membrane.8

Figure S6: Pore size distribution of **PVC** and **TETA-PVC** membranes9

Figure S7: Water contact angle values of (a) **PVC** and (b) **TETA-PVC**9

Figure S8: EDX analysis of **TETA-PVC** membrane after adsorption11

Figure S9: SEM images of **PVC** and **TETA-PVC** membranes after adsorption11

Figure S10: Freundlich isotherm plots for **TETA-PVC** membrane14

Figure S11: SEM images of **TETA-PVC** membrane used to treat water with different concentrations of **Pb(II)** ions.14

Figure S12: SEM images of **PVC** and **TETA-PVC** membranes in a tertiary system of **Hg(II), Pb(II), and Cd(II)**15

Figure S13: Removal efficiency of 10 mg of **PVC** and **TETA-PVC** membranes in a mixed metal ions system of **Pb(II), Hg(II), and Cd(II), As(III), Cu(II), and Zn(II)** ([M] = 150 mg/L each).....16

Figure S14: EDX analysis of **TETA-PVC** membrane after desorption16

List of tables

Table S1: Surface parameters—thickness and pore size distribution8

Table S2: Percentage removal of unfunctionalised and functionalised electrospun membranes within 24 hours.....10

Table S3: The value of parameters in the kinetic models (K_1 : rate constant; q_e : quantity adsorbed at equilibrium; R^2 : coefficient of determination) (**Pb(II)** concentration = 150 mg/L, amount of adsorbent (**PVC-TETA** = 0.01 g, solution pH = 7, time = 10 to 1440 min, volume = 10 mL and temperature = 25°C) .12

Table S4: Adsorption isotherm model parameters13

1. General

1.1. Chemicals and materials

All chemicals and reagents used in this study were of analytical grade, obtained from commercial suppliers, and used without further purification unless otherwise noted. Polyvinyl chloride (PVC) with a molecular weight of 80,000 g/mol and a density of 1.4 g/mL, dimethylformamide (DMF) with $\geq 99.8\%$ purity, tetrahydrofuran (THF) with $\geq 99.9\%$ purity, triethylenetetramine (**TETA**) with a molecular weight of 146.23 g/mol and a density of 0.982 g/mL, and **lead(II)** acetate trihydrate $\text{Pb}(\text{OAc})_2 \cdot 3\text{H}_2\text{O}$ were all purchased from Sigma. Commercial nylon screen fabric with an average pore size diameter of 350 μm and thickness of $215 \pm 2 \mu\text{m}$ was used as a support for the electrospun membranes.

1.2. Instruments and methods

Agilent 8453 UV-visible spectrophotometer using a 1 cm path length was used to detect the absorption spectra of the samples, which were placed in a quartz cuvette for analysis. Samples of **lead(II)**, **TETA**, and **TETA-lead(II)** mixture solutions were analyzed under ambient conditions instantaneously. Polyvinyl chloride membrane was synthesized using a laboratory-scale electrospinning machine (FLUIDNATEK LE-10, BIOINICIA, Spain) and further functionalised with an organic ligand (**TETA**). Functionalised and unfunctionalised membranes were fully characterised using FTIR, SEM, EDX, and TGA. FTIR spectra (4 scans, 4 cm^{-1} resolution, wave number range $4000 - 650 \text{ cm}^{-1}$) were obtained using a Perkin Elmer FTIR Spectrum 2000 Spectrophotometer with a diamond/ZnSe crystal window. Scanning electron microscopy (SEM) and energy dispersive X-ray (EDX) imaging were performed using MIRA3 Tescan electron microscope after the samples were coated with a 20 nm thin layer of platinum. Moreover, thermal stabilities of the electrospun **PVC** membranes were measured using thermogravimetric analysis (TGA), which was performed using a Netzsch TG 209 F1 Libra apparatus. Samples were heated from 30 to 800 $^{\circ}\text{C}$ at a heating rate of 10 K min^{-1} . The average pore size of the membranes was also measured using a capillary flow porometer CFP-1100- from Porous Material Inc. (PMI), USA, along with the water contact angle to detect the hydrophilicity/hydrophobicity of both membranes using optical tensiometer (OCA 15EC, DataPhysics, Germany) with a droplet volume of 5 μm . As for the removal efficiency, the decrease in the concentration of **lead(II)** was detected by an atomic absorption spectrometer (AAS), iCE 3000 series.

2. Metal-organic complex detection using UV-visible spectroscopy

2.1. Metal-organic complex detection

In this study, the chelation of **Pb(II)** ions to triethylenetetramine (**TETA**) organic ligand in water to form a metal-organic complex was investigated using UV-visible spectrophotometer. Prior to investigating the metal-organic complex, the concentration of **Pb(II)** and **TETA** in water was optimized separately. A solution rich in **lead(II)** ions (**lead(II)** acetate trihydrate) was prepared (representing contaminated water). **TETA** solution was also prepared and added to the lead induced water to validate the complexation of **Pb(II)** ions with **TETA**. Absorption spectra of different mixtures of lead and TETA with different concentrations were recorded at room temperature with no waiting time to detect the formation of the metal-organic complex. Absorption spectra of **TETA**, **Pb(II)**, and **TETA - Pb(II)** complex spectra are presented in **Figure S1**. The concentrations tested were within the acceptable range of absorbance ($0.1 < \text{Abs} < 2.7$). A maximum absorption peak for **Pb(II)** ions is detected at 208 nm; whereas the maximum absorption band for the ligand was observed at a wavelength of 190 nm.

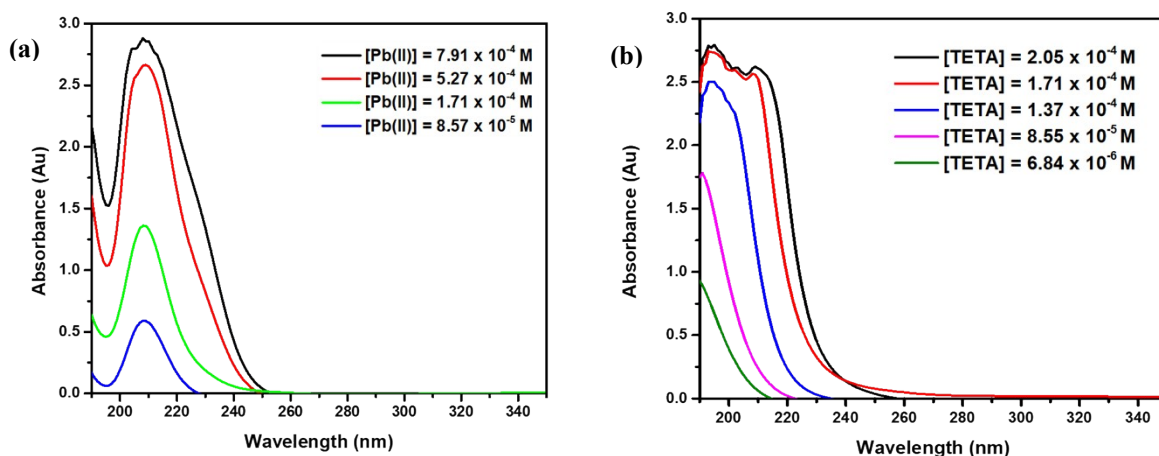


Figure S1: Absorption spectrum of **Pb(II)** and **TETA** in aqueous solutions:(a), **lead(II)** acetate trihydrate within the UV-visible region (b) triethylenetetramine within the UV-visible region

2.2. Binding isotherm of **lead(II)** ion and **TETA**

A titration was carried out to assess the binding strength and stoichiometry of the metal and ligand, where different concentrations of the ligand were titrated to a solution rich in **Pb(II)** of constant concentration (1.71×10^{-4} M) in water. The titration was carried out in a 15 mL conical tube and the resulting solution was placed in the UV spectrophotometer cuvette for testing, under same ambient conditions. A gradual addition of **TETA** to the **Pb(II)** aqueous solution within a concentration range of 0 to 1.71×10^{-4} M was performed and analyzed using the UV-vis spectrophotometer instantaneously.

Higher concentrations were also tested (**Figure S2**) to assess the stoichiometry and binding constant of the complex. The experimental data was fitted using **EQN S1**, representing a 1:1 binding mode.¹

$$y = Y_0 + D_Y \times \frac{((K_a \times (P + x) + 1) - (((K_a \times (P + x) + 1)^2) - 4 \times K_a^2 \times P \times x)^{1/2})}{(2 \times K_a \times P)}$$

(S1)

Where Y is the absorbance of the complex, Y₀ is the initial absorbance, P is the concentration of the metal, D_Y is the change in absorbance, and K_a is the binding association/ constant.

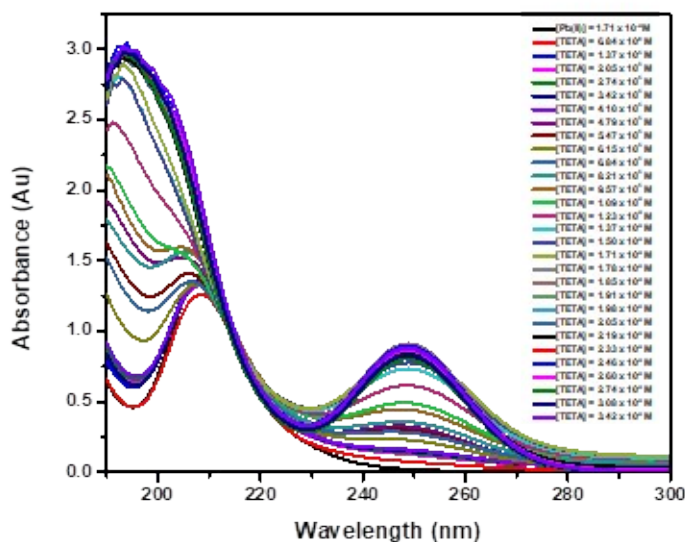


Figure S2: UV-visible absorption spectra of 1.71×10^{-4} M solution of **Pb(OAc)₂** in H₂O titrated with, increasing concentrations of **TETA**

3. Synthesis and functionalisation of PVC membrane

An electrospun polymer membrane was fabricated to serve as a solid support for the organic ligand in order to capture **lead(II)** ions from water. The polymer used in this study is polyvinylchloride (PVC), which is the 3rd most widely used polymer characterised by its chemical stability and ability to be functionalised. A polymeric solution of **PVC** was prepared and injected in an electrospinning machine to prepare the desirable nanofibrous membrane. For the preparation of the polymeric solution, using THF alone as the solvent showed undesirable results where a wrinkly surface structure was formed due to the high volatility of the solvent. In order to avoid this problem, DMF, a non-volatile solvent, was mixed with

THF to reduce the evaporation time while the solution is being ejected. The fibers produced by mixing both solvents showed a better morphology and high mechanical strength. A solvent ratio of 62.5:37.5/DMF:THF was reported to produce the optimal morphology of the fiber. The solvent was prepared by mixing 7 mL of DMF with 4 mL of THF. The optimal **PVC** polymer concentration was 16% by weight resulting the highest fiber diameter, 1.936 g of **PVC** was added to the solvent. The solution was left on a stirrer at a speed of 700 rpm at room temperature. The electrospinning machine was used to fabricate the **PVC** membrane using the polymeric solution prepared under a fixed electric field of 18 kV. After that, the electrospun **PVC** membrane was placed into a solution of **TETA** and ethanol of different ratios of **PVC** (mg) to **TETA** (μL) (1:1, 1:2, 1:3) for surface modification. The reaction was set at 65°C for 5 hours. The membrane was then washed with ethanol and distilled water before leaving it to dry at room temperature.

4. Characterisation of PVC and TETA-PVC membranes

4.1. Fourier-transform infrared spectroscopy

Fourier-transform infrared spectroscopy (FTIR) spectroscopy was used to characterise the chemical composition of the nanofibrous membranes and to validate the modification process of the **PVC** membrane by detecting the presence of the amine bond formed between **TETA** and the membrane. It was also used to detect the complexation of TETA to Pb(II) ions after adsorption.

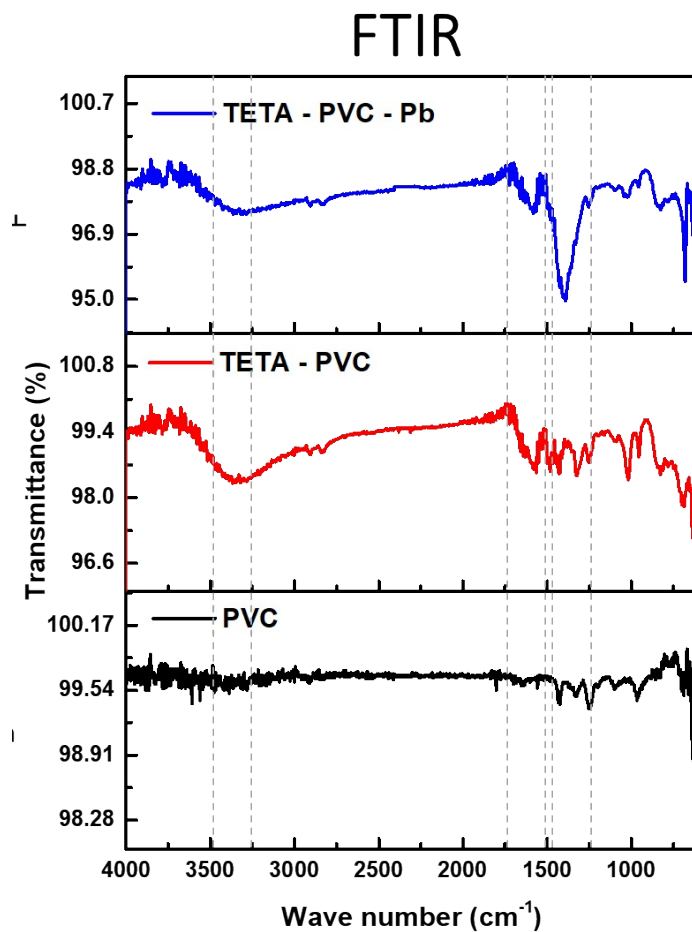


Figure S3: FTIR spectra of **PVC**, **TETA-PVC**, and **TETA-PVC-Pb** membranes

4.2. Scanning Electron Microscopy

Scanning Electron Microscopy (SEM) was used to study the surface characteristics of the **PVC** membrane before and after modification for the three different **PVC**: **TETA** ratios. SEM images show that the fibers' morphology has changed upon modification.

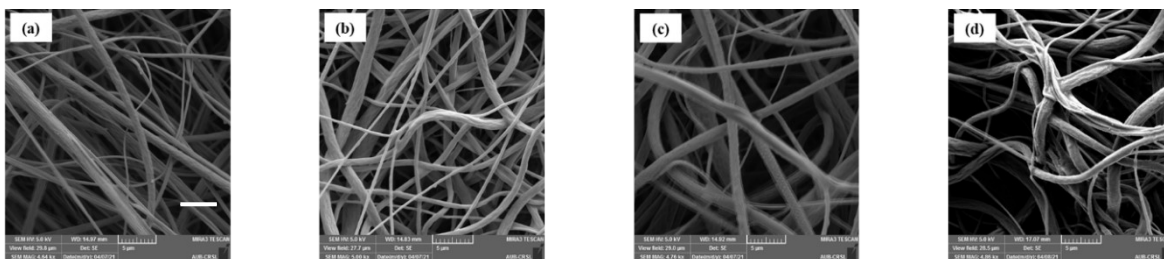


Figure S4: SEM images of electrospun **PVC** nanofibers obtained from different **PVC** (g): **TETA** (mL) ratios (a) unfunctionalised **PVC** membrane; (b) 1:1, (c) 1:2, and (d) 1:3 ratios.

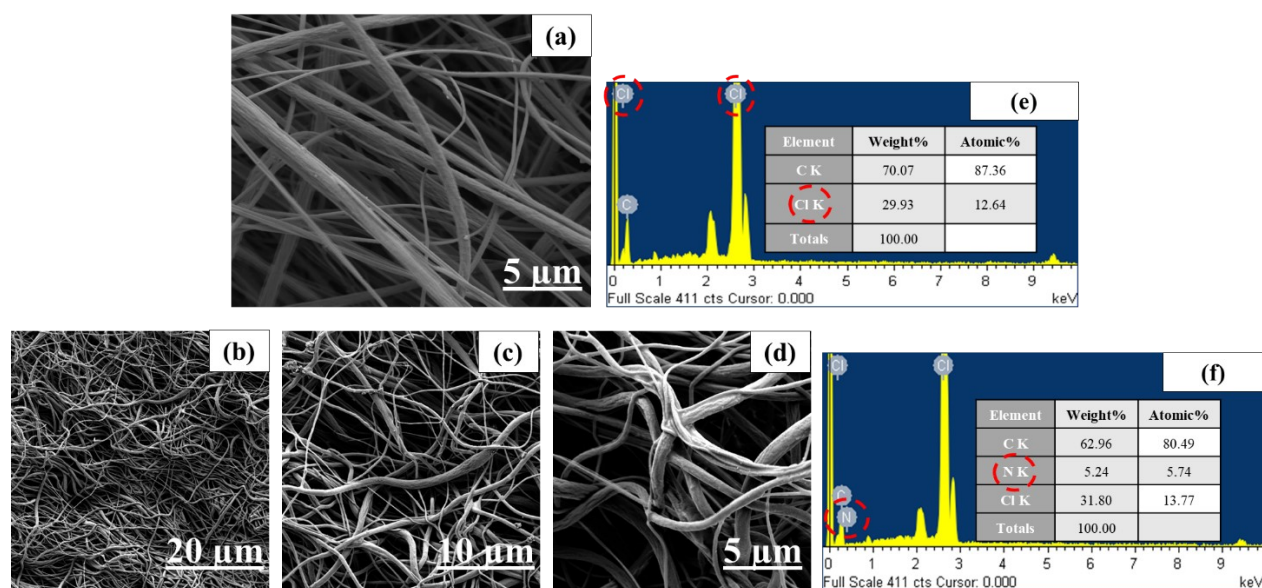


Figure S5: SEM images of PVC nanofibers membrane and TETA-PVC nanofibers membrane with different magnifications: unfunctionalised PVC (a) 5 μm, TETA-PVC (b) 20 μm; (c) 10 μm; (d) 5 μm. EDX analysis of (e) PVC membrane; (f) TETA-PVC membrane.

4.3. Energy Dispersive X-ray

Energy Dispersive X-ray (EDX) analysis was performed on the membrane to identify the elemental composition of the membrane and to provide a quantitative analysis of the elements detected in the sample. Peaks corresponding nitrogen were observed by the EDX spectrum.

4.4. Pore size, membrane thickness, and water contact angle measurements

The average pore size was measured using a capillary flow porometer CFP-1100- from Porous Material Inc. (PMI), USA. In order to measure the average pore size, a membrane sample was horizontally sandwiched in the sample chamber, saturated with a wetting liquid, then properly sealed. Afterward, air is passed into the chamber at an increasing differential pressure. When the pressure reaches an adequate level to overcome the capillary action of the fluid in the largest pore, the fluid is displaced in that pore. The corresponding pressure is the bubble point. The pressure is increased further until the liquid in all pores is displaced and the sample is considered dry. Meanwhile, the flow rate and gas pressure are monitored in order to generate the pore size distribution and mean pore size diameter.

Table S1: Surface parameters—thickness and pore size distribution

Membrane	Mean flow pore diameter (μm)	Average thickness (nm)
PVC	3.575	105 \pm 11
TETA-PVC	3.201	144 \pm 24

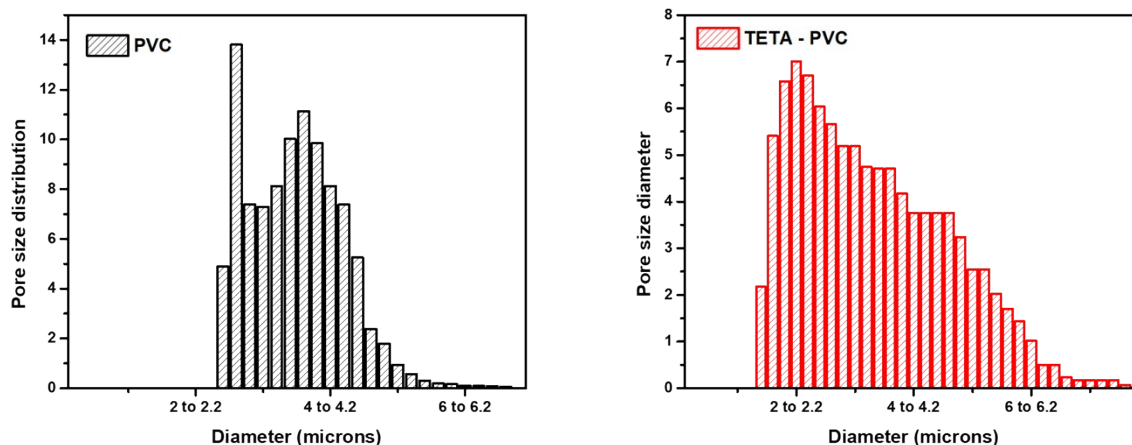


Figure S6: Pore size distribution of **PVC** and **TETA-PVC** membranes

The contact angle is a quantitative measure of the wettability of a surface or material (wetting of a solid by a liquid). A water droplet with a contact angle over 90 degrees indicates a hydrophobic surface and less than 90 degrees indicates a hydrophilic surface.² The water contact angle (WCA) was measured using an optical tensiometer (OCA 15EC, DataPhysics, Germany) with a water droplet volume of 5 μm . A sample of **TETA-PVC** and **PVC** membranes was placed on the sample holder and then a droplet of water from a syringe provided in the tensiometer was carefully dropped on the membrane. The measurements were repeated five times for each sample and the contact angle was averaged.

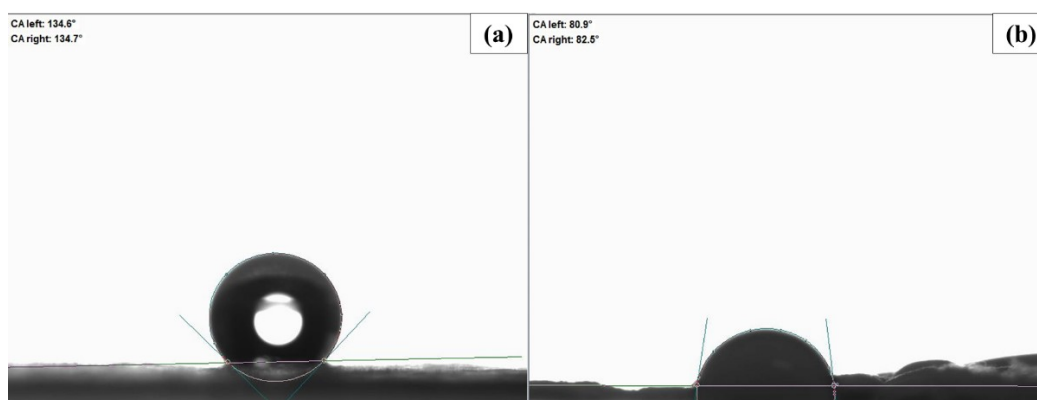


Figure S7: Water contact angle values of (a) **PVC** and (b) **TETA-PVC**

5. Removal efficiency of **Pb(II)** ions from water

PVC and **TETA-PVC** membranes were tested for the removal of **lead(II)** from water at ambient conditions (neutral pH and room temperature). Atomic absorption spectroscopy (AAS) was used to monitor the change in the concentration of **Pb(II)** ions in water before and after treatment with both membranes. Four different **PVC** membranes were immersed in 150 mg/L **lead(II)** solution to study the removal efficiency. Sample 1 was treated with the unfunctionalised **PVC** membrane, samples 2 to 4 were treated with functionalised **PVC** membranes with 1:1, 1:2, and 1:3 ratio of **PVC** (g) to **TETA** (mL), respectively. The samples were subjected to the same conditions where they were left in the shaker at a speed of 100 rpm and at room temperature. Aliquots were taken from the four samples after being in contact in the solution for 0.5, 1, 2, and 24 hours, then analyzed using the AAS. The percentage removal was calculated according to the following equation:

$$Removal (\%) = \frac{(C_i - C_e)}{C_i} \times 100 \quad (S2)$$

Where: C_i is the initial concentration (mg/L) of metal ions in solution, C_e is the equilibrium concentration (mg/L) of metal ions in solution.

Table S2: Percentage removal of unfunctionalised and functionalised electrospun membranes within 24 hours

PVC (g): TETA (ml)	% Removal of Pb(II) at different time(hr) slots			
	0.5 hr	1 hr	2 hr	24 hr
1:0	6.76	18.41	23.70	43.49
1:1	31.71	33.35	36.39	48.73
1:2	73.26	77.26	80.17	81.68
1:3	88.61	89.63	87.90	81.80

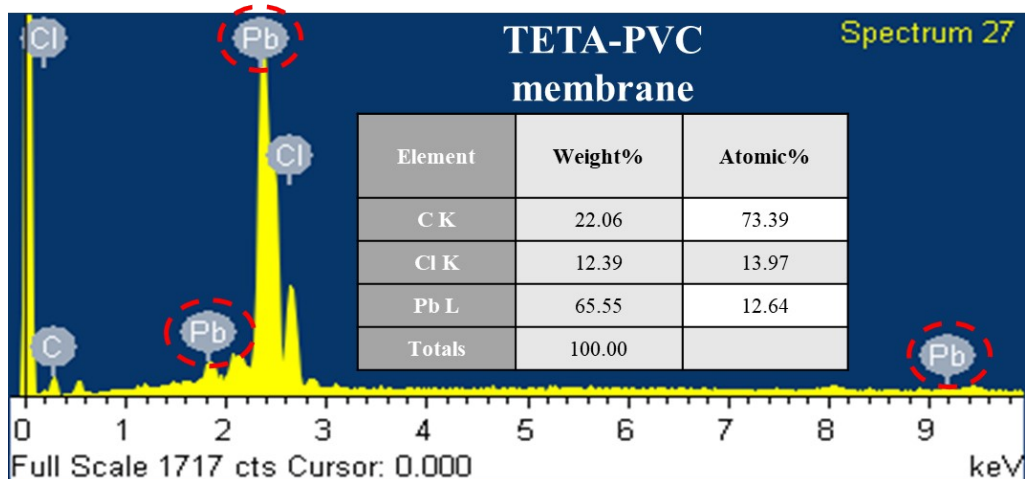


Figure S8: EDX analysis of TETA-PVC membrane after adsorption

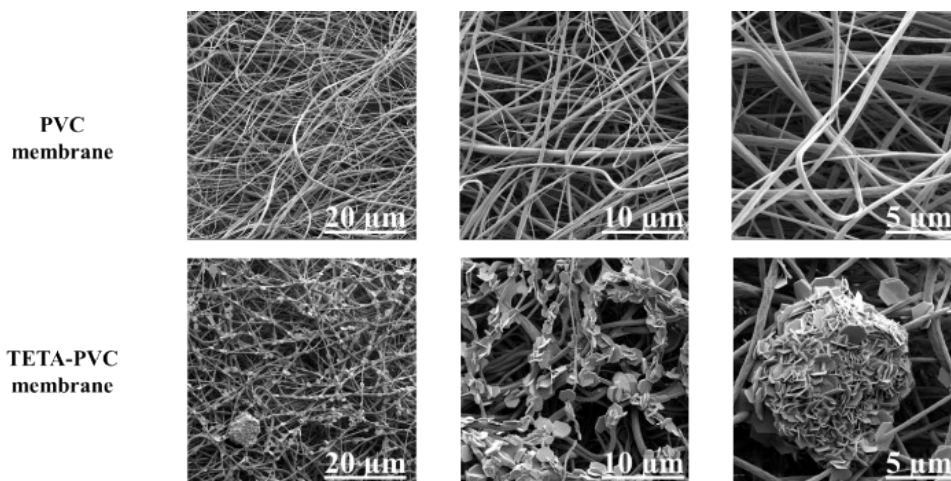


Figure S9: SEM images of PVC and TETA-PVC membranes after adsorption

6. Adsorption Kinetics

The kinetic data were fitted with the pseudo-second-order kinetic model using the following equation (EQN S3):³

$$\frac{t}{qt} = \frac{1}{K_2 q_e^2} + \frac{t}{q_e} \quad (\text{S3})$$

Where q_e (mg/g) and qt (mg/g) are the amount of **Pb(II)** metal ions adsorbed at equilibrium and at time t (min), respectively; t (min) is adsorption time and k_2 (g/mg/min) is the pseudo-second-order adsorption rate constant.

Table S3: The value of parameters in the kinetic models (K_1 : rate constant; q_e : quantity adsorbed at equilibrium; R^2 : coefficient of determination) (**Pb(II)** concentration = 150 mg/L, amount of adsorbent (**PVC-TETA** = 0.01 g, solution pH = 7, time = 10 to 1440 min, volume = 10 mL and temperature = 25°C)

Model	Parameters	[Pb(II)] mg/L
Pseudo-first order	K_1 (min ⁻¹) q_e (cal) (mg/g) R^2	8×10^{-5} 8.302×10^{-3} 0.2246
Pseudo-second order	K_2 (min ⁻¹) q_e (cal) (mg/g) R^2	1.02×10^{-2} 120.48 0.9999

7. Adsorption Isotherm models

Adsorption equilibrium experiments were carried out with different initial concentrations of **lead(II)** ions as 600, 700, 900, 1000, and 1,200 mg/L to assess the interaction between the adsorbate (**Pb(II)**) and the adsorbent (**TETA-PVC**). 10 mg of the **TETA-PVC** membrane was immersed in each of the prepared **Pb(II)** aqueous solutions and left in the shaker at a speed of 100 rpm at room temperature for 30 minutes. Aliquots were taken from the solutions, filtered separately through a 0.45 μm filter syringe and analyzed by AAS. The amount of adsorbed metal ion at equilibrium, q_e (mg/g) was calculated by **EQN S4**:⁴

$$q_e = \frac{(C_i - C_e)v}{w} \quad (\text{S4})$$

Where C_i and C_e (mg/L) are the initial and equilibrium concentrations of metal ion, respectively. Volume of the solution V (L), and W is the mass of **TETA-PVC** (g). The experimental data were fitted into Langmuir and Freundlich isotherm models,⁵⁻⁷ which are mathematical models that give a description about the distribution of the adsorbate and adsorbent in aqueous solution according to the heterogeneity/homogeneity of the adsorbent, coverage type and interaction between the adsorbate species.

7.1. Langmuir isotherm model

The Langmuir equation verifies a monolayer interaction between the adsorbate molecules on to the surface of the adsorbent. The linear form of this isotherm is represented by the expression:⁵

$$\frac{C_e}{q_e} = \frac{C_e}{q_{max}} + \frac{1}{q_{max}k_L} \quad (\text{S5})$$

Where q_e (mg/g) and C_e (mg/L) are the amount of adsorbed metal ions per unit weight of adsorbent and concentration of metal ions in solution at equilibrium, respectively. The constant K_L (L/g) is the Langmuir equilibrium constant related to the energy of adsorption and q_{max} is maximum adsorption capacity (mg/g). The essential feature of the Langmuir isotherm can be expressed in terms of a dimensionless constant called separation factor (R_L , also called equilibrium parameter) which is defined by the following equation:

$$R_L = \frac{1}{1 + K_L C_0} \quad (S6)$$

Where C_0 (mg/L) is the initial adsorbate concentration. The value of R_L indicates the shape of the isotherms to be either unfavorable ($R_L > 1$), linear ($R_L = 1$), favorable ($0 < R_L < 1$) or irreversible ($R_L = 0$).

7.2. Freundlich isotherm model

The most important multisite adsorption isotherm for heterogeneous surfaces is the Freundlich adsorption isotherm and the linear form of this isotherm is expressed as:⁷

$$\log q_e = \log k_f + \frac{1}{n} \log C_e \quad (S7)$$

Where q_e is the metal uptake (mg/g) at equilibrium, K_f is the measure of the sorption capacity, $1/n$ is the sorption intensity, and C_e is the final ion concentration in solution, or equilibrium concentration (mg/L). The Freundlich isotherm constants K_f and $1/n$ are evaluated from the intercept and the slope, respectively of the linear plot of $\log q_e$ versus $\log C_e$.

The value of n reflects the type of isotherm to be favorable ($0 < 1/n < 1$), irreversible ($1/n = 0$) or unfavorable ($1/n > 1$).

Table S4: Adsorption isotherm model parameters

Langmuir and Freundlich model parameters for adsorption of Pb(II) ions on TETA-PVC

Langmuir model		Freundlich model	
R^2	0.992	R^2	0.895
K_L (L/mg)	0.409	K_f (mg/g)	0.422
R_L	0.002-0.004	$1/n$	0.256

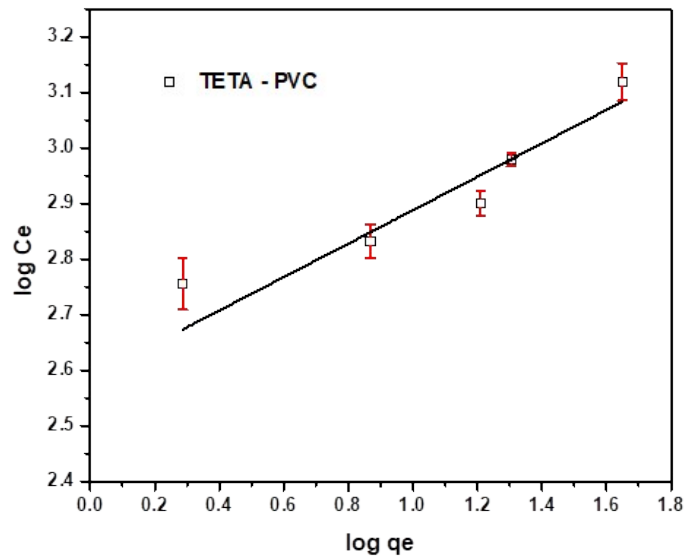


Figure S10: Freundlich isotherm plots for TETA-PVC membrane

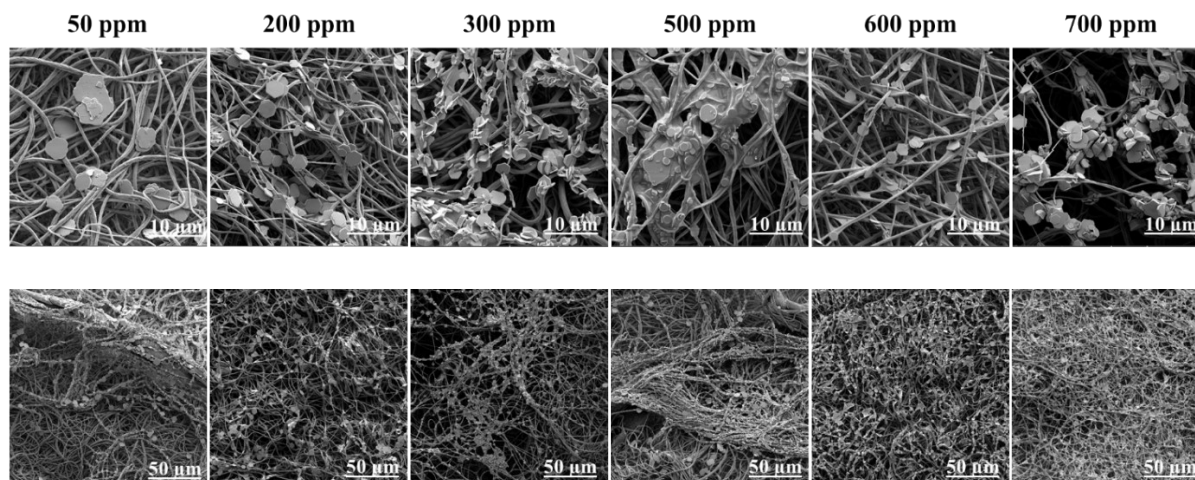


Figure S11: SEM images of TETA-PVC membrane used to treat water with different concentrations of Pb(II) ions.

8. Ion selectivity test

8.1. Tertiary System

The competitive adsorption of Pb(II), Cd(II), and Hg(II) with TETA-PVC and PVC membranes was studied. The experiment was conducted through immersing 10 mg of TETA-PVC membrane in a solution containing equal concentration (150 mg/L) of Hg(II), Cd(II), and Pb(II) ions. The samples were left in the shaker at a speed of 100 rpm at ambient conditions for 30 minutes. The interference effect of the foreign ions on the removal efficiency was investigated compared to the single component solution. The samples were collected, filtered, then the concentration of each

metal ion was tested using AAS. The adsorption tests were performed in duplicate, representing the error bars and average values.

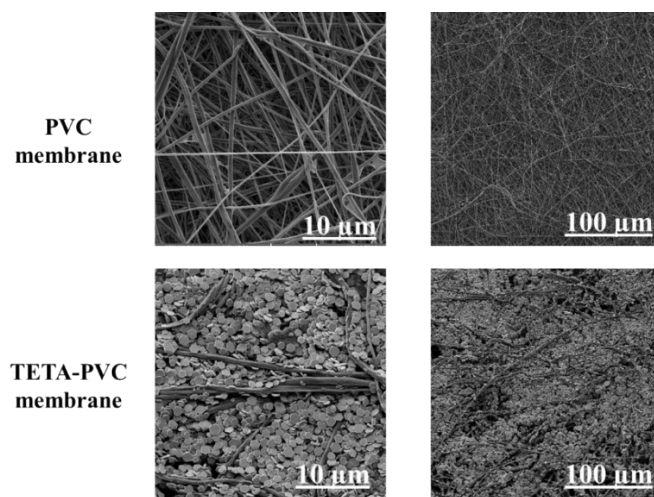


Figure S12: SEM images of **PVC** and **TETA-PVC** membranes in a tertiary system of **Hg(II)**, **Pb(II)**, and **Cd(II)**

8.2. Mixed Metal Ions System

The competitive adsorption of **Pb(II)**, **Hg(II)**, **Cd(II)**, **As(III)**, **Zn(II)**, and **Cu(II)** with **TETA-PVC** and **PVC** membranes was studied. The experiment was conducted through immersing 10 mg of **TETA-PVC** membrane in a solution containing equal concentration (150 mg/L) of the six metal ions. The samples were left in the shaker at a speed of 100 rpm at ambient conditions for 30 minutes. The interference effect of the foreign ions on the removal efficiency was investigated compared to the single component solution. The samples were collected, filtered, then the concentration of each metal ion was tested using AAS. As can be observed, in the mixed solution of metal ions, the removal percentage of the pristine **PVC** membrane towards all metals is relatively low (**less than 35%**), with the highest removal percentage towards **Zn(II)** ions ($\approx 17\%$). Whereas in the presence of the six different cations, the removal of **lead(II)** by the **TETA-PVC** membrane was still the highest ($\approx 77\%$) (**Figure S13**). The selectivity of metal ions for the **TETA-PVC** membrane was in the order of **Pb(II) > Zn(II) > As(III) > Hg(II) > Cd(II) > Cu(II)**.

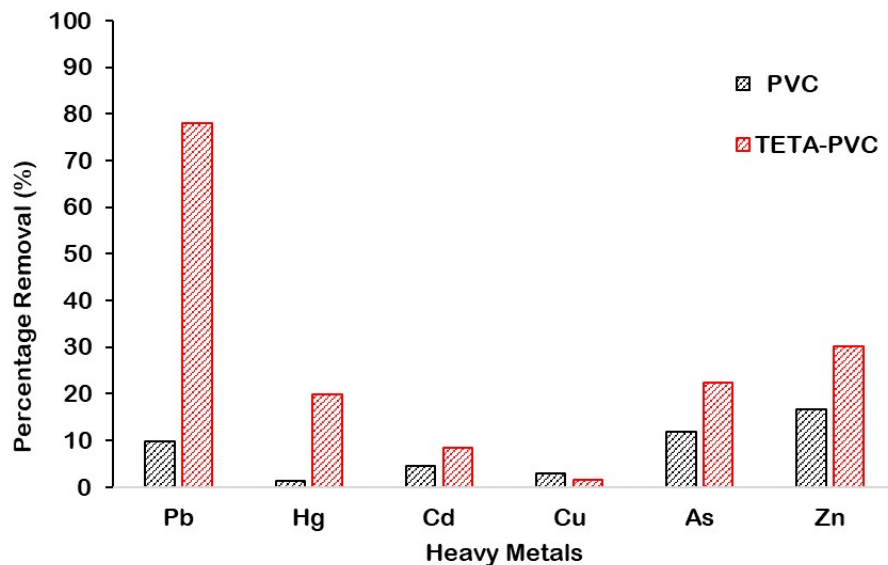


Figure S13: Removal efficiency of 10 mg of PVC and TETA-PVC membranes in a mixed metal ions system of **Pb(II)**, **Hg(II)**, and **Cd(II)**, **As(III)**, **Cu(II)**, and **Zn(II)** ([M] = 150 mg/L each)

9. Regeneration of TETA-PVC membrane

The potential reusability of **TETA-PVC** under mild acidic conditions was tested with *p*-toluene sulfonic acid (0.1 M). 10 mg of the membrane was immersed in 10 mL water containing 700 mg/L **Pb(II)** (pH = 7), which was then placed in a shaker set at 100 rpm at room temperature, for 30 minutes. The removal of **lead(II)** ions by the membrane was analysed using AAS. The membrane was then treated with 0.1 M *p*-toluene sulfonic acid solution (pH= 5-6) to regenerate the adsorbent. The regenerated **TETA-PVC** was washed with distilled water to be used in another cycle of **Pb(II)** removal. This process was repeated six times.

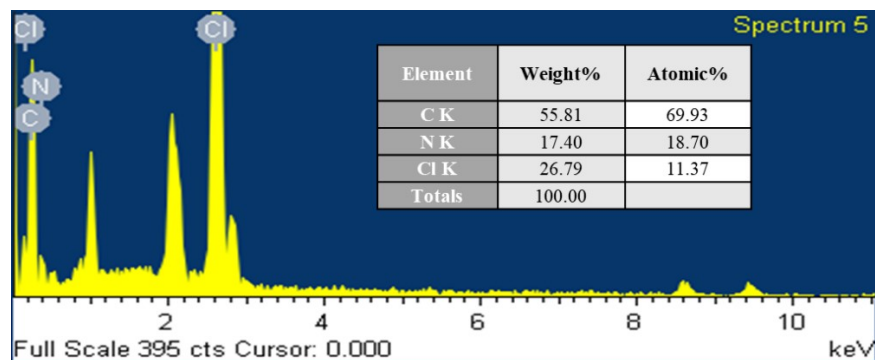


Figure S14: EDX analysis of **TETA-PVC** membrane after desorption

List of References

- 1 F. Zapata, A. Caballero, A. Espinosa, A. Tárraga and P. Molina, *J. Org. Chem.*, 2009, **74**, 4787–4796.
- 2 S. Parvate, P. Dixit and S. Chattopadhyay, *J. Phys. Chem. B*, 2020, **124**, 1323–1360.
- 3 D. Yang, L. Li, B. Chen, S. Shi, J. Nie and G. Ma, *Polymer*, 2019, **163**, 74–85.
- 4 K. T. Aung, S.-H. Hong, S.-J. Park and C.-G. Lee, *Applied Sciences*, 2020, **10**, 1738.
- 5 M. B. Desta, *Journal of Thermodynamics*, 2013, **2013**, e375830.
- 6 T. S. Khayyun and A. H. Mseer, *Appl Water Sci*, 2019, **9**, 170.
- 7 A. Mittal, L. Kurup and J. Mittal, *Journal of Hazardous Materials*, 2007, **146**, 243–248.